

Article

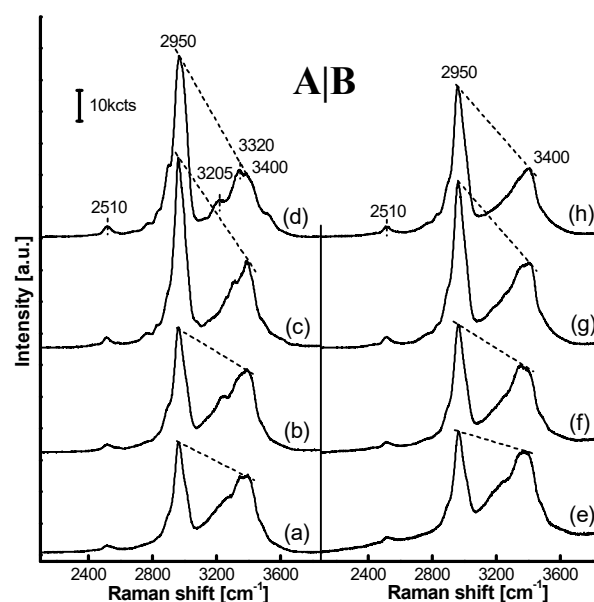
# SERRS Detection on Silver Nanoparticles Supported on Acid-Treated Melamine-Resin Microspheres

Chaofeng Duan <sup>1</sup>, Lu Shen <sup>1</sup>, Yuqing Guo <sup>1</sup>, Xiaogang Wang <sup>1</sup>, Xiaohua Wang <sup>2</sup> and Zhixian Hao <sup>1,\*</sup>

<sup>1</sup> Shanghai Key Laboratory of Chemical Assessment and Sustainability, School of Chemical Science and Engineering, Tongji University, Shanghai 200092, China; 1831027@tongji.edu.cn (C.D.); Shenlu218@163.com (L.S.); superyq@tongji.edu.cn (Y.G.); xgwang@tongji.edu.cn (X.W.)

<sup>2</sup> Institute of Industrial Catalysis, Zhejiang University of Technology, Hangzhou 310014, China; wangxiaohua0909@163.com

\* Correspondence: haozhixian@tongji.edu.cn; Tel.: +86-13761772106



**Citation:** Duan, C.; Shen, L.; Guo, Y.; Wang, X.; Wang, X.; Hao, Z. SERRS Detection on Silver Nanoparticles Supported on Acid-Treated Melamine Resin-Microspheres. *Nanomaterials* **2021**, *11*, 1337. <https://doi.org/10.3390/nano11051337>

Received: 30 March 2021

Accepted: 10 May 2021

Published: 19 May 2021

**Publisher's Note:** MDPI stays neutral with regard to jurisdictional claims in published maps and institutional affiliations.



**Copyright:** © 2021 by the authors. Submitted for possible open access publication under the terms and conditions of the Creative Commons Attribution (CC BY) license (<http://creativecommons.org/licenses/by/4.0/>).

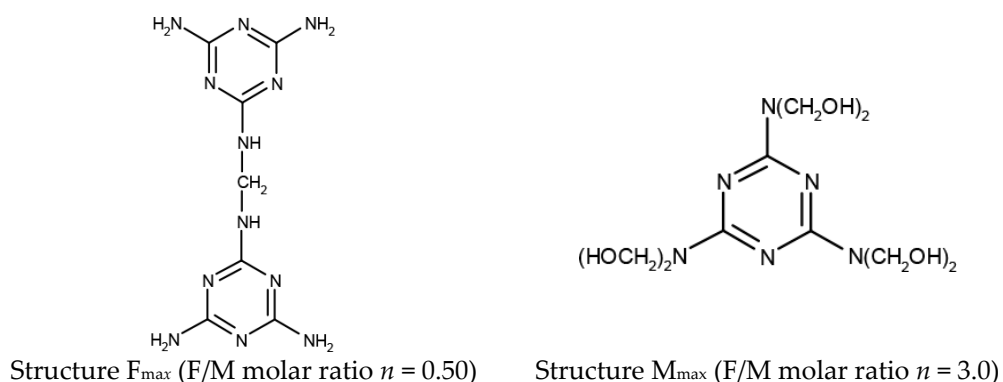
**Figure S1.** Impact of the acid-treatment on Raman spectra of MF<sub>*n*</sub> microspheres. (a): MF<sub>2</sub>, (b): MF<sub>3</sub>, (c): MF<sub>6</sub> and (d): MF<sub>9</sub> in (A) were collected on non-treated microspheres, while (e): MF<sub>2</sub>, (f): MF<sub>3</sub>, (g): MF<sub>6</sub> and (h): MF<sub>9</sub> in (B) were collected on the acid-treated microspheres. An increasing parameter (*n*) enhanced the Raman scattering peak at 2950 cm<sup>-1</sup> while the slope value between two scattering peaks (2950 and 3400 cm<sup>-1</sup>) of each MF<sub>*n*</sub> sample declined due to the acid-treatment reaction.

Figure S1A and B respectively show the Raman spectra of MF<sub>*n*</sub> microspheres and the microspheres after the acid-treatment reaction. A strong Raman scattering band at 2950 cm<sup>-1</sup> and a medium wide one at around 3400 cm<sup>-1</sup> were due to the stretching vibrations of C–H and N–H that were attributed to the formaldehyde and melamine that had been added to the MF<sub>*n*</sub> synthetic-reaction, respectively. The intensity ratio between the two bands, shown as a slope for each sample, was enhanced when the parameter (*n*) increased from 2.00 to 9.00 as shown from Figure S1A (a) to (d). This finding implies that there was a progressive addition of formaldehyde into the MF<sub>*n*</sub> microspheres as the parameter (*n*) increased. Furthermore, the intensity ratio for each sample declined after the acid-treatment reaction, as shown by the peak slope from each sample in Figure 2A being higher than that from the sample with the same parameter (*n*) in Figure S1B. This suggests that the removed mass portion, more than 4.29 wt% as shown in Table 1, consisted of MF<sub>*n*</sub> oligomers with more terminal –NHCH<sub>2</sub>OH groups. In addition, the Raman scattering band pattern at around 3400 cm<sup>-1</sup> on each non-treated MF<sub>*n*</sub> sample was complicated when

compared to that on the acid-treated sample. Scattering peaks at 3205 and 3320  $\text{cm}^{-1}$  appeared faint after the acid-treatment reaction. This implied that oligomers had been removed during the acid-treatment reaction.

### 1. F/M Molar Ratio Present in $\text{MF}_n$ Polymer Structure

According to the valence bond theory, one molecule of formaldehyde combines two molecules of melamine at most in the molecular structure and one molecule of melamine needs six molecules of formaldehyde, as shown in Figure S2. Any possible F/M molar ratio in  $\text{MF}_n$  polymer structures could thus be schemed out between the values 0.50 and 3.0 existent in Structures  $\text{F}_{\text{max}}$  and  $\text{M}_{\text{max}}$ , respectively.



**Figure S2.** Two extreme structures in  $\text{MF}_n$  polymers.

For example, various linear  $\text{MF}_n$  polymers with the F/M molar ratio between 1.0 and 2.0 in Structures  $\text{L}_1$  and  $\text{L}_2$  in Figure S3 could be constructed, based on the  $-\text{NH}_2$  side substitution with  $-\text{NHCH}_2\text{OH}$  groups in different degrees.

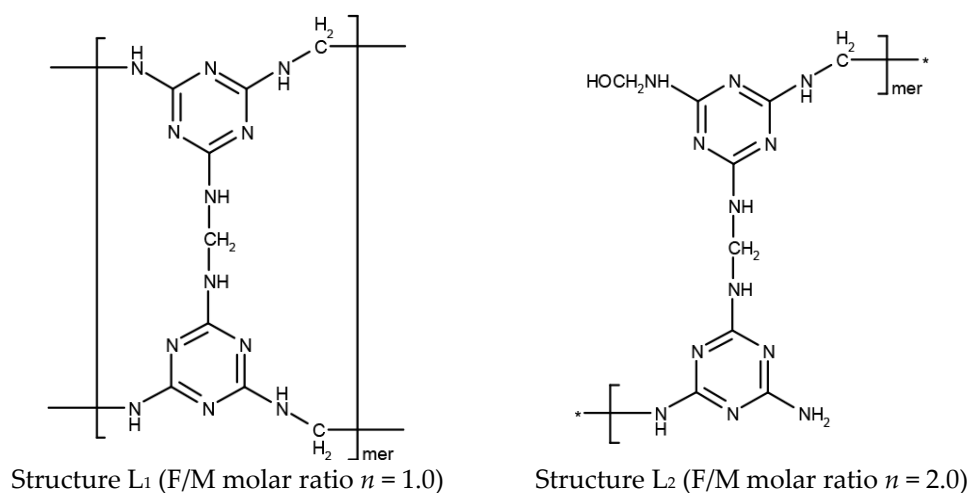


**Figure S3.** Two extreme structures in linear  $\text{MF}_n$  polymers. Wherein, all the  $-\text{NH}_2$  groups in the melamine structure are substituted by  $-\text{NHCH}_2-$ .

### 2. F/M Molar Ratio $n$ Adopted in the Synthetic-Reaction, as well as Excess Monomer

The F/M molar ratio, i.e. the experiment parameter ( $n$ ), in the synthetic-reaction for  $\text{MF}_n$  polymers is another concept, which is hardly consistent with the F/M molar ratio ( $n$ ) present in the resultant polymer structure. It is possible to synthesize  $\text{MF}_n$  microspheres at the parameter  $n = 9.0$ , a value that is more than the maximum F/M molar ratio  $n = 6.0$  in the Structure  $\text{M}_{\text{max}}$  as shown in Figure S2. Even so, this excess formaldehyde in the synthetic-reaction was found to be crucial rather than useless. A concept "excess monomer" [26] was thus claimed to emphasize the impact of the parameter  $n$  on characteristics of the

resultant polymers. The excess monomer was verified to be able to influence various characteristics of the UF resin microspheres, e.g. output, solubility, crystallinity, nucleation, density and water absorption of UF resin microspheres, as reported in our previous work [26].

### 3. The Boundary Characteristics and Terminal Overreaction of Excess Monomer

According to the parameter ( $n$ ), characteristics of the  $MF_n$  polymers are classifiable. The SERRS signals will gain intensity if the synthetic-reaction for the  $MF_n$  microspheres incorporated in the substrate is kept for 9.0 h with the parameter  $n$  more than 1.5, and otherwise it will be frustrate [27]. A similar phenomenon also occurred on the SERRS substrate incorporating UF microspheres, where the F/U molar ratio was more than 1.0 [26]. Obviously, the parameter  $n = 1.5$  indeed acts as a boundary between two different SERRS performances of the substrate, on which the excess monomers are able to be divided into two regions for identification of the substrate performance. The parameter  $n = 1.5$  is associated with two ideal units in  $MF_n$  structures as shown as Structure  $L_{mer}$  and  $T_{mer}$  in Figure S4, in which all  $-NH_2$  are substituted by  $-NHCH_2-$  groups or one  $-NH_2$  group remained.

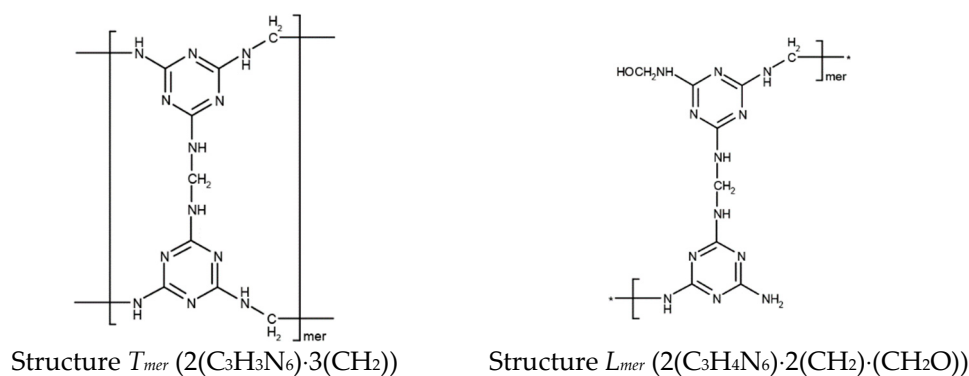


**Figure S4.** Two ideal units in linear  $MF_n$  polymer structure with the F/M molar ratio  $n = 1.5$ .

The ideal unit Structure  $T_{mer}$  could extend in one, two or three-dimensions based on consistent  $-NHCH_2-$  groups, except for the terminal sites as shown as Structures L,  $P_9$  and  $T_{72}$  in Figure S7, S8 and S9. Formulas of  $MF_n$  polymers from it in one, two and three-dimensions are as following.

$$\text{Formula L: } [2(C_3H_3N_6)3(CH_2)]_x \cdot 2H_2O \quad (\text{linear}) \quad (1)$$

$$\text{Formula P: } [2(C_3H_3N_6)3(CH_2)]_{xy} \cdot (2x + y - 1)(H_2O) \quad (\text{planar}) \quad (2)$$

$$\text{Formula T: } [2(C_3H_3N_6)3(CH_2)]_{xyz} \cdot z(2x + y - 1)(H_2O) \quad (3D) \quad (3)$$

Herein, the three-dimensional structure of Formula T is from overlay of the planar structure of Formula P in a lamellar way. The parameters  $x$ ,  $y$ ,  $z$  are also the numbers of replications in  $x$ -,  $y$ - and  $z$ -axis directions and the polymerization degree  $m$  equals  $x$ ,  $xy$ , and  $xyz$  in linear, planar and three-dimensional structures, respectively.

The terminal overreaction of excess monomer emphasize a fact that the linear molecule  $AB(AB)_m A$  from excess monomer A in the synthetic-reaction, for example, is different with the molecule  $B(AB)_m AB$  from excess monomer B. For the linear, planar, and three-dimensional  $MF_n$  polymers, the terminal overreactions with excess formaldehyde are shown as following Equations.

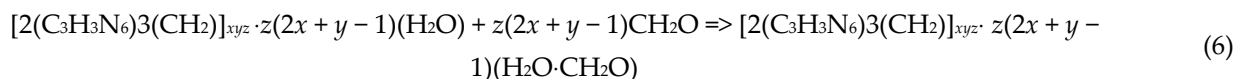
Equation LO (linear)



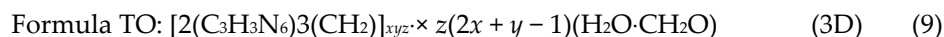
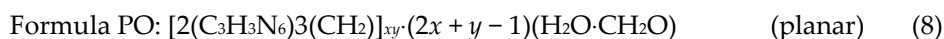
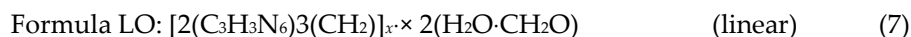
Equation PO (planar)



Equation TO (3D)



After the terminal overreaction, Formula L, P and T are transferred into Formula LO, PO and TO as following.



These equations demonstrate that the excess monomer, e.g. excess formaldehyde, will further concentrate at the end of a linear polymer molecule, around a planar molecule or on the surfaces of a three-dimensional one under ideal structural conditions. Further demonstration of these overreactions is presented at the end of context, as Equations L<sub>m</sub>, P<sub>9</sub> and T<sub>72</sub> as shown in Figure S10, S11 and S12, respectively.

#### 4. Influence of Polymerization Degree $m$ on the F/M Molar Ratio $n$ Present in MF <sub>$n$</sub> Polymers

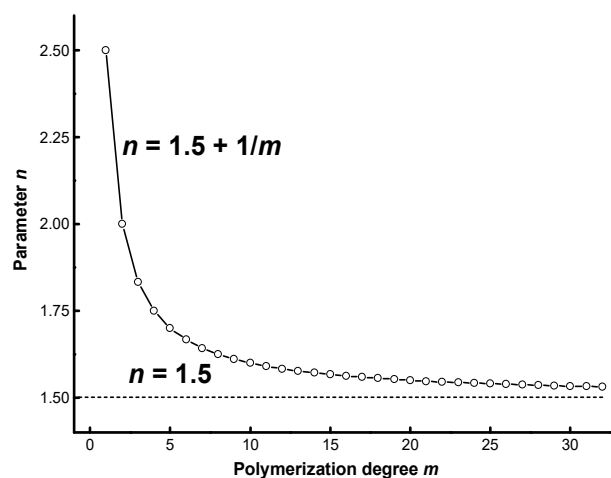
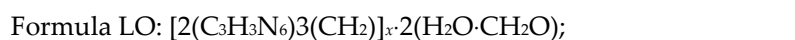


**Figure S5.** Influence of polymerization degree  $m$  on the F/M molar ratio  $n$  in an ideal linear polymer structure.



The F/M molar ratio  $n = 1.5 + (1/x) = 1.5 + (1/m)$

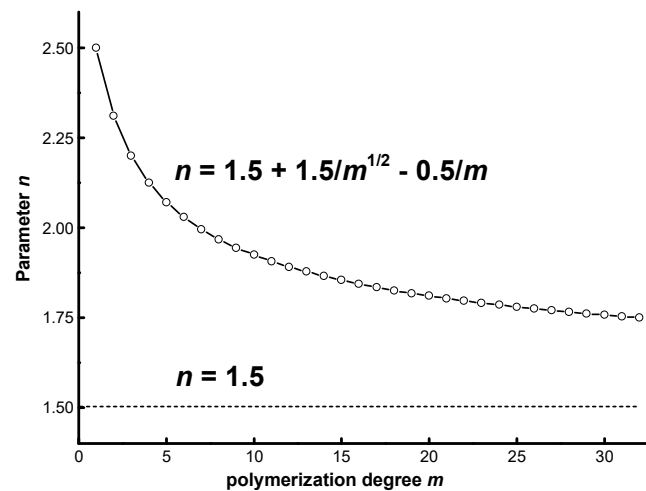
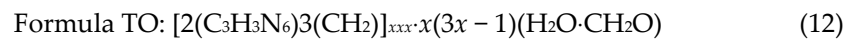
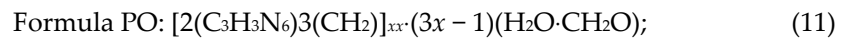


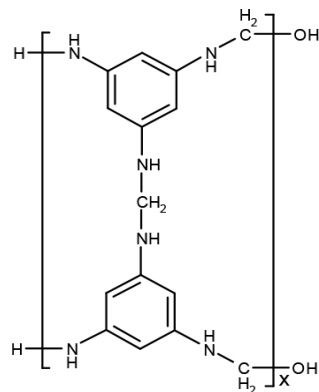
**Figure S6.** Influence of polymerization degree  $m$  on the F/M molar ratio  $n$  in the planar or three-dimensional structures.



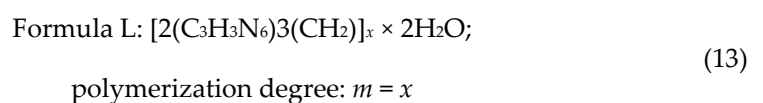
Provided the  $x = y = z$ , the F/M molar ratio  $n = 1.5 + 1.5/x^2 - 0.5/x = 1.5 + 1.5/m^{1/2} - 0.5/m$ . The same function for Formulas PO and TO because Structure TO is from the lamellar overlay of Structure PO.

Influences of polymerization degree  $m$  on the F/M molar ratio  $n$  in one-, two- and three-dimensional structures are shown in Figure S5 and S6. Obviously, the F/M molar ratio  $n$  in  $\text{MF}_n$  polymers increases with the polymerization degree  $m$  decreasing under an excess formaldehyde condition, especially rapidly in the two- and three-dimensional cases.

### 5. Three Ideal Types of $\text{MF}_n$ Polymer Structures and Their Terminal Overreactions



**Figure S7.** Linear structure of an  $\text{MF}_n$  polymer molecule (Structure L).  $x$  is the degree of polymerization.



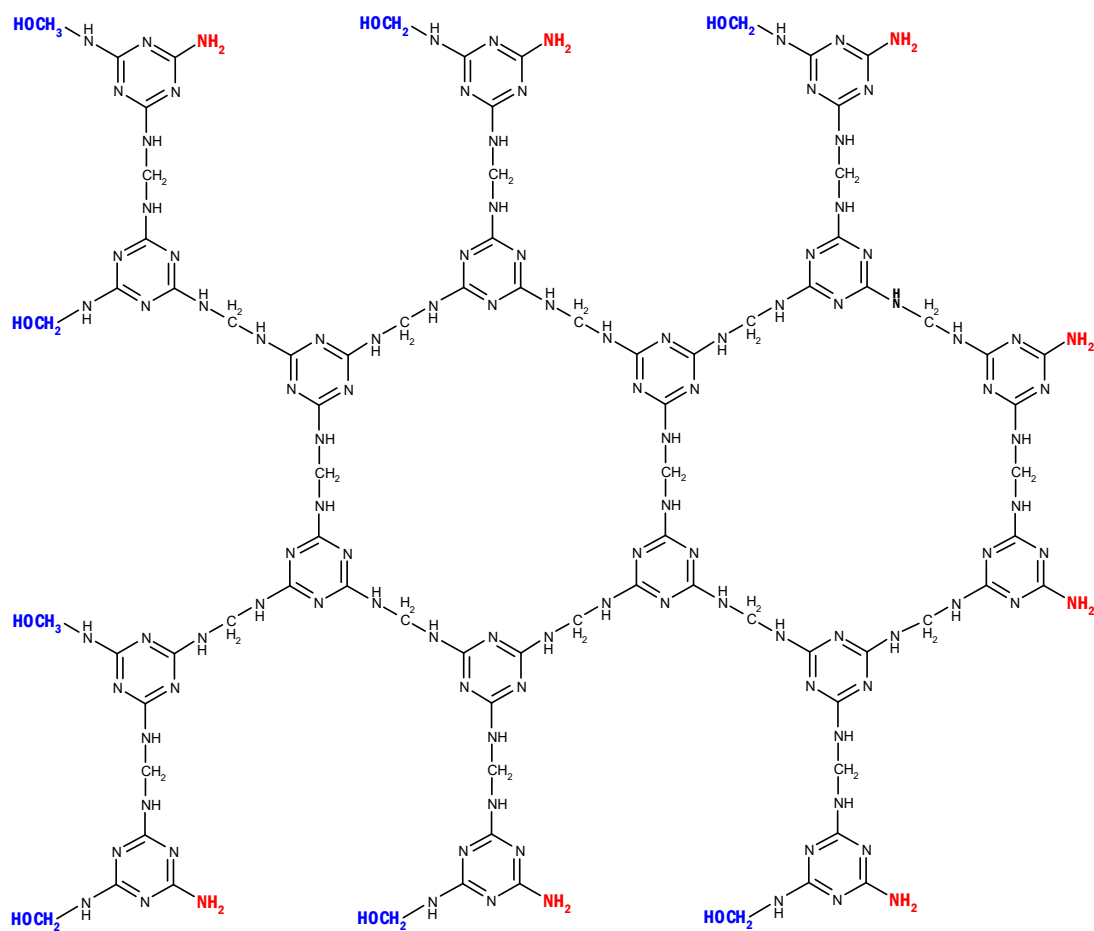


Figure S8. Planar structure of an MF<sub>n</sub> nonamer (Structure P<sub>9</sub>).

$$\text{Formula P}_9: [2(\text{C}_3\text{H}_3\text{N}_6)_3(\text{CH}_2)]_9 8(\text{H}_2\text{O}); x = y = 3;$$

$$\text{polymerization degree: } m = xy = 9$$

(14)

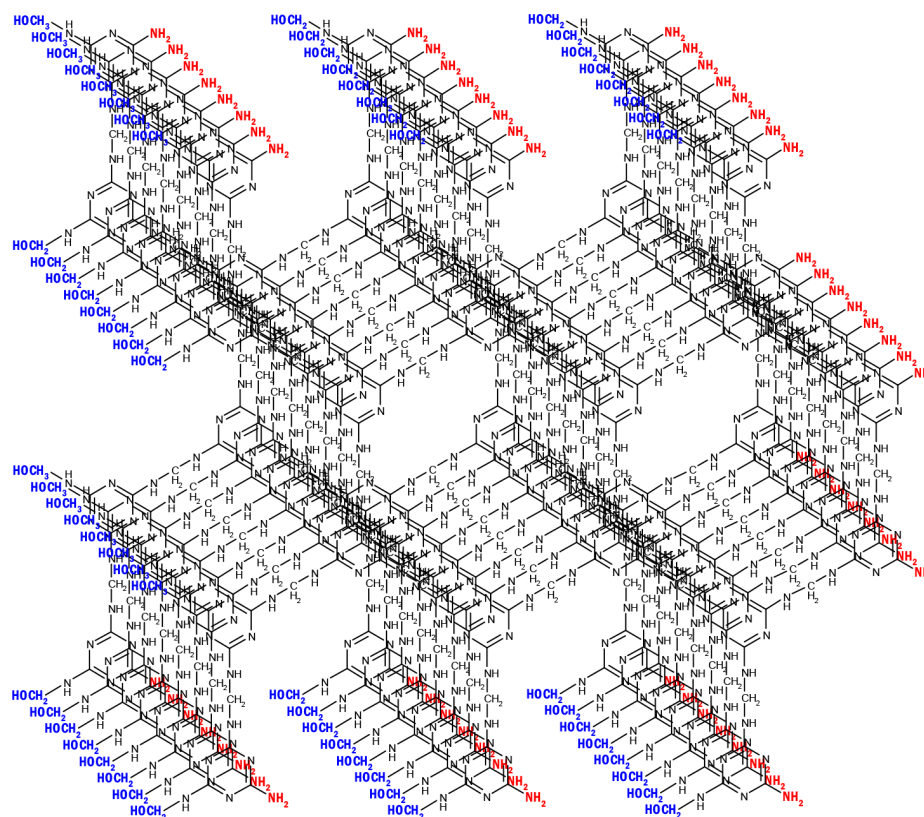


Figure S9. Three-dimensional structure of an MF<sub>n</sub> seventy-two polymer (Structure T<sub>72</sub>).

$$\text{Formula T}_{72}: [2(\text{C}_3\text{H}_3\text{N}_6)_3(\text{CH}_2)]_{72} 64(\text{H}_2\text{O}); x = y = 3; z = 8;$$

$$\text{polymerization degree } m = xyz = 72$$

(15)

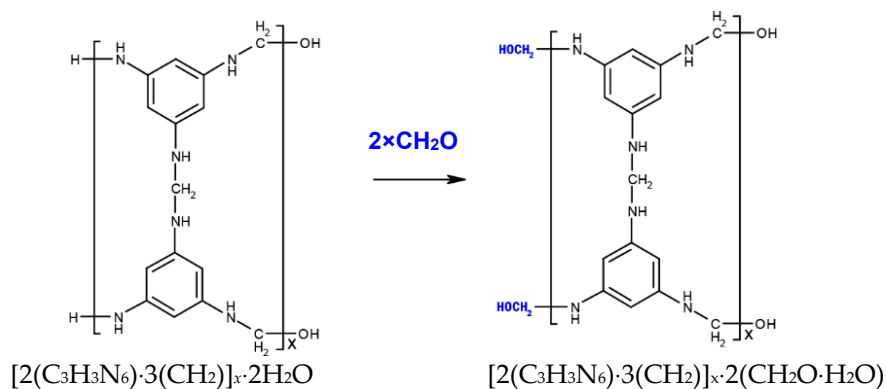
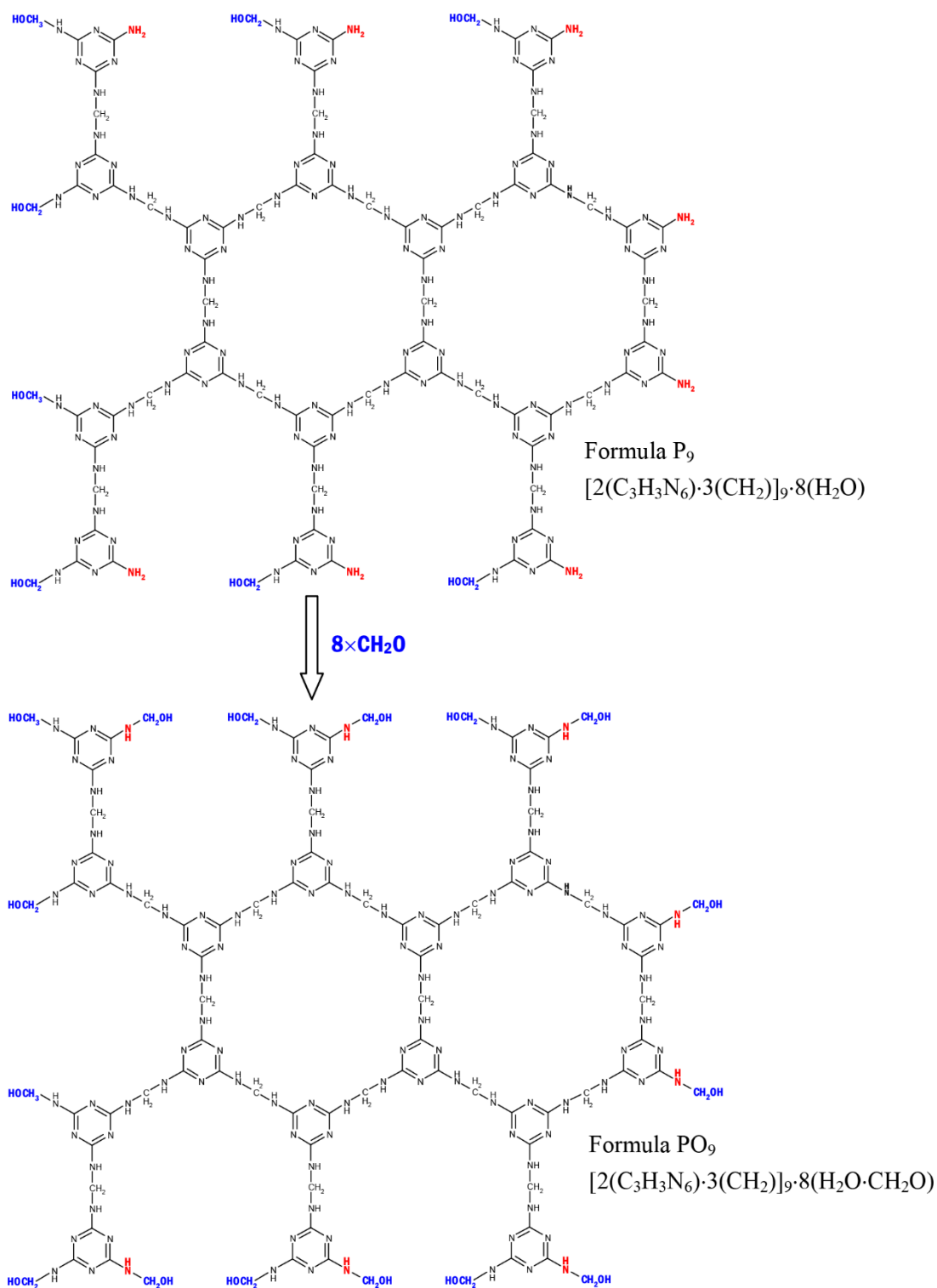
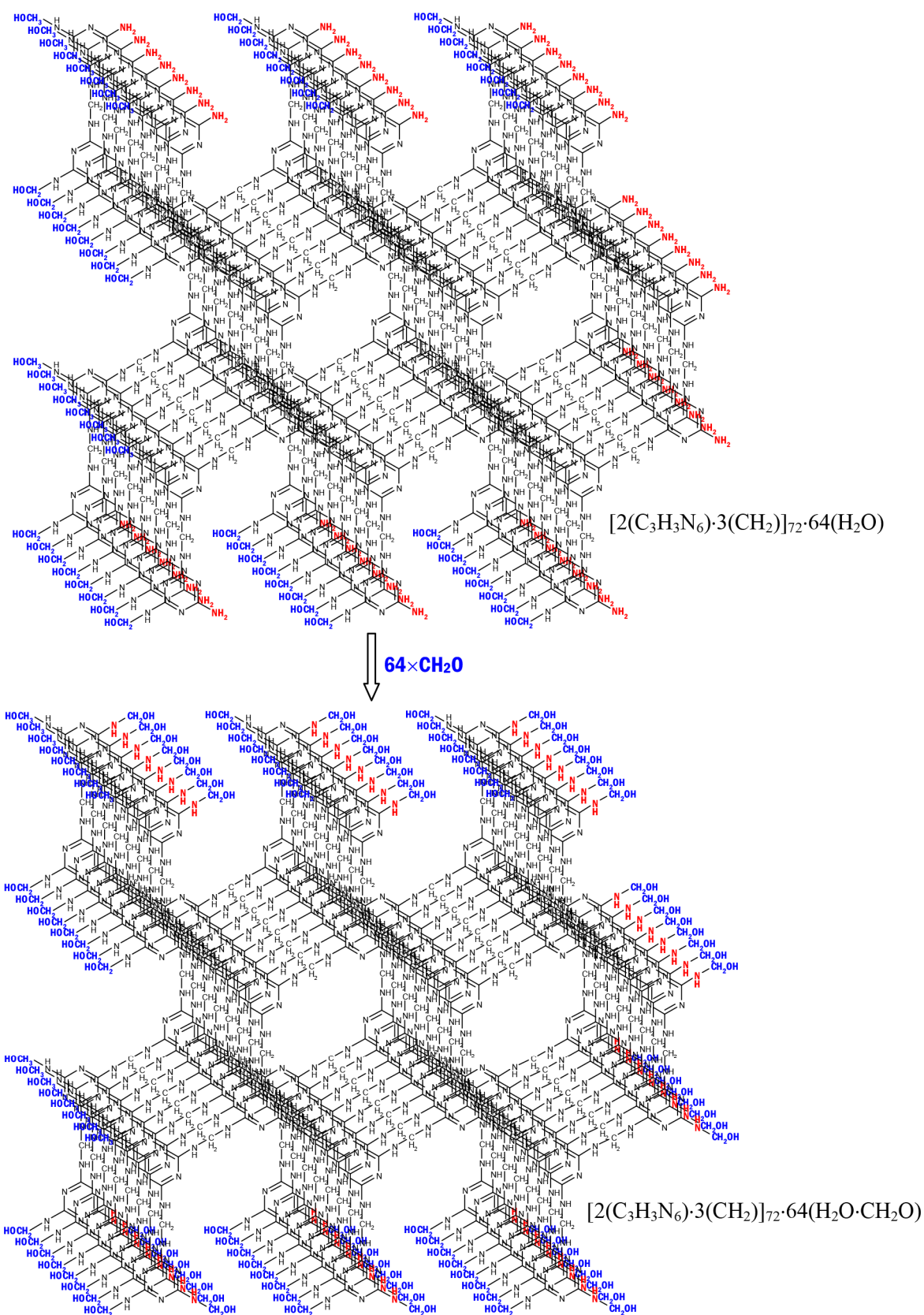


Figure S10. Terminal overreaction at the end of a linear MF<sub>n</sub> molecule (Equation LO); polymerization degree  $m = x$ .



**Figure S11.** Terminal overreaction at the end of a planar MF<sub>7</sub> nonamer (Equation P<sub>9</sub>);  $x = y = 3$ ; polymerization degree  $m = xy = 9$ .



**Figure S12.** Terminal overreaction at the end of a three-dimensional MF<sub>n</sub> seventy-two polymers (Equation T72)  $x = y = 3$ ,  $z = 8$ ; polymerization degree  $m = xyz = 72$ .

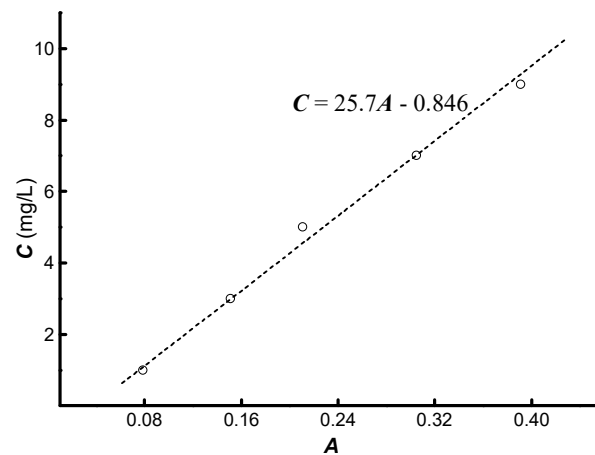


**Figure S13.** Silver concentration as a function of absorbance from spectrophotometry.

The working curve:  $C = 25.7A - 0.846$  (mg/L), for which the wavelength 400 nm was adopted

In order to acquire the AgNP content in AgNP/MF<sub>3</sub>, 100 mg MF<sub>3</sub> was added in 10.0 mL AgNP colloid solution with a silver concentration 5.00 mg/L and let settlement for 1 h following a 5 min ultrasound treatment. The mixture was then separated at a centrifugal rate of 6000 rpm for 5 min. AgNP concentrations in the initial AgNP colloid solution and the residual colloid liquor after the AgNP adsorption were both measured on absorption spectrophotometry, respectively. The silver content in the AgNP/MF<sub>3</sub> was calculated and summarized in Table S1.

**Table S1.** Calculation of silver content in the AgNP/MF<sub>3</sub>.\*

	incorporating no-treated MF <sub>3</sub>			incorporating acid-treated MF <sub>3</sub>		
	A	C(mg/L)	m(mg)	A	C (mg/L)	m(mg)
colloid before adsorption	0.227	5.00	0.0500	0.227	5.00	0.0500
colloid after adsorption	0.192	4.09	0.0409	0.205	4.42	0.0442
Ag adsorbed from 10.0 mL colloid	0.0500 - 0.0409 = 0.0091 (mg)			0.0500 - 0.0442 = 0.0058 (mg)		
Ag content in 100 mg AgNP/MF <sub>3</sub>	0.0091 (mg)/100 (mg)= 91 × 10 <sup>-6</sup>			0.0068 (mg)/100 (mg)=58 × 10 <sup>-6</sup>		

\* The silver concentration of the colloid solution:  $C = 25.7A - 0.846$  (mg/L); The silver amount in the 10.0 mL colloid solution:  $m = C \times 10.0 \times 10^{-3}$ (mg).

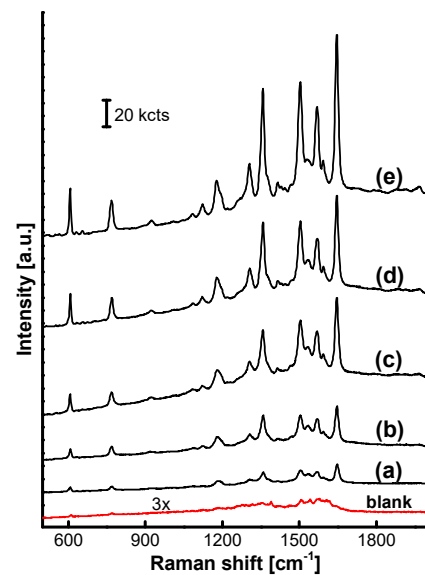


**Figure S14.** SERS performance of AgNPs treated with the liquor from MF<sub>6</sub> acid-treatment reaction. (a) 20, (b) 40, (c) 60, (d) 80 and (e) 100 °C were collected on the AgNPs that were treated with liquors from the MF<sub>6</sub> acid-treatment reaction at varied temperatures from 20 to 100 °C and a laser power of 0.01 mW. The blank AgNPs was examined at a laser power of 0.05 mW and its R6G-SERS signal was magnified 3 times as shown at the bottom. SERS signals on the AgNPs had their intensities gradually enhanced with the MF<sub>6</sub> acid-treatment temperature increased.

Figure S14 shows the R6G-SERS performance of AgNPs treated with the liquor from the MF<sub>6</sub> acid-treatment reaction. The R6G SERS signal was enhanced with the acid-treatment temperature gradually increased from 0 to 100 °C. These results were on the contrary with those obtained on the AgNP/MF<sub>6</sub> where the incorporating MF<sub>6</sub> from the same acid-treatment reactions executed at the varied temperature from 40 to 100 °C. It was obvious that the oligomers in the MF<sub>n</sub> microspheres had transferred into the hydrolyzed liquor and played an important role in the construction of SERS hotspots.

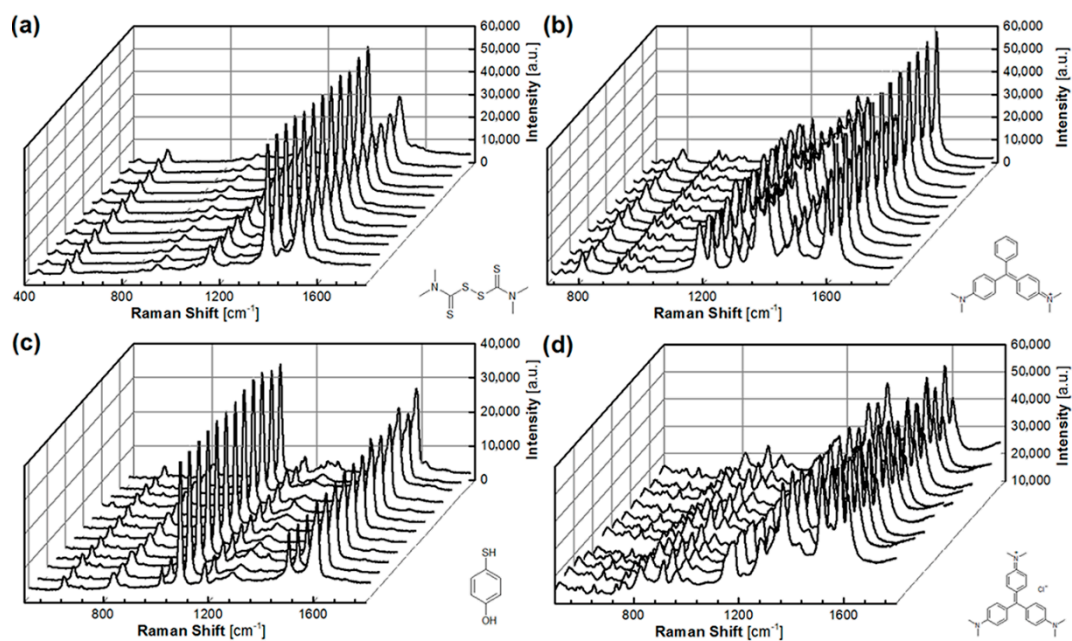


**Figure S15.** SERS spectra of a set of analytes collected on AgNP/MF<sub>6</sub> substrate. (a) Tetramethylthiuram disulfide, (b) malachite green, (c) p-hydroxythiophenol and (d) basic violet 14 were collected on substrate incorporating MF<sub>6</sub> microspheres, synthesized at pH 4.0 and 65 °C for 20 min, acid-treated at pH 4.0 and 40 °C for 10 min, where twelve spectra for statistic analysis of each analyte were randomly collected on different microspheres of the SERS substrate.

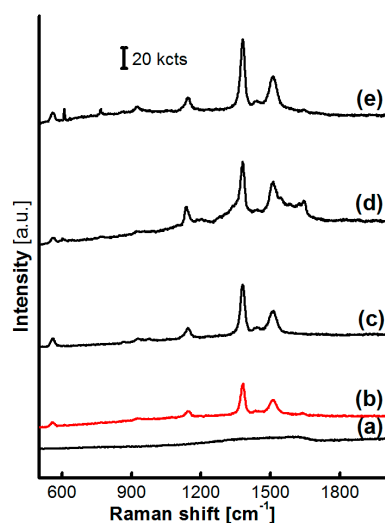


**Figure S16.** SERRS spectrum as a function of the tetramethylthiuram disulfide concentration on the optimized AgNP/MF<sub>6</sub>. (a)  $1.0 \times 10^{-9}$ , (b)  $1.0 \times 10^{-8}$ , (c)  $1.0 \times 10^{-7}$ , (d)  $1.0 \times 10^{-6}$  and (e)  $1.0 \times 10^{-5}$  M were tetramethylthiuram disulfide -SERRS spectra on the optimized AgNP/MF<sub>6</sub> treated with a tetramethylthiuram disulfide solution from  $1.0 \times 10^{-9}$  to  $1.0 \times 10^{-5}$  M tetramethylthiuram disulfide at a laser power of 0.01 mW. The tetramethylthiuram disulfide SERRS spectrum was still clear if the AgNP/MF<sub>6</sub> was treated with a  $1.0 \times 10^{-8}$  M tetramethylthiuram disulfide solution.

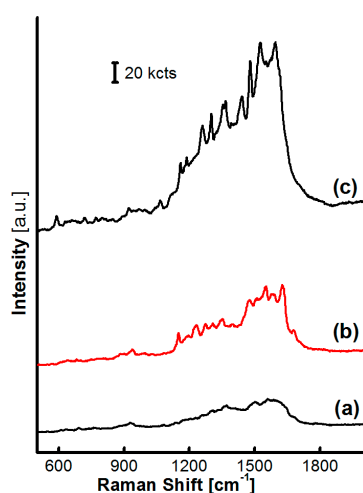


**Figure S17.** SERRS spectrum as a function of the malachite green concentration on the optimized AgNP/MF<sub>6</sub>. (a)  $1.0 \times 10^{-8}$ , (b)  $1.0 \times 10^{-7}$  and (c)  $1.0 \times 10^{-6}$  M were malachite green-SERRS spectra on the optimized AgNP/MF<sub>6</sub> treated with a malachite green solution from  $1.0 \times 10^{-8}$  to  $1.0 \times 10^{-6}$  M malachite green at a laser power of 0.01 mW. The malachite green SERRS spectrum was clearest if the AgNP/MF<sub>6</sub> was treated with a  $1.0 \times 10^{-6}$  M concentration malachite green solution.

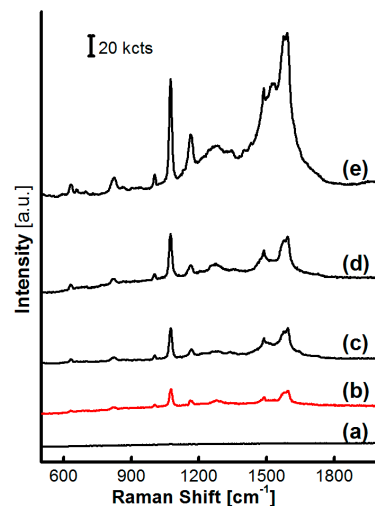


**Figure S18.** SERRS spectrum as a function of the p-hydroxythiophenol concentration on the optimized AgNP/MF<sub>6</sub>. (a)  $1.0 \times 10^{-8}$ , (b)  $1.0 \times 10^{-7}$ , (c)  $1.0 \times 10^{-6}$ , (d)  $1.0 \times 10^{-5}$  and (e)  $1.0 \times 10^{-4}$  M were p-hydroxythiophenol-SERRS spectra on the optimized AgNP/MF<sub>6</sub> treated with a p-hydroxythiophenol solution from  $1.0 \times 10^{-8}$  to  $1.0 \times 10^{-4}$  M p-hydroxythiophenol at a laser power of 0.01 mW. The p-hydroxythiophenol SERRS spectrum was still clear if the AgNP/MF<sub>6</sub> was treated with a  $1.0 \times 10^{-7}$  M p-hydroxythiophenol solution.

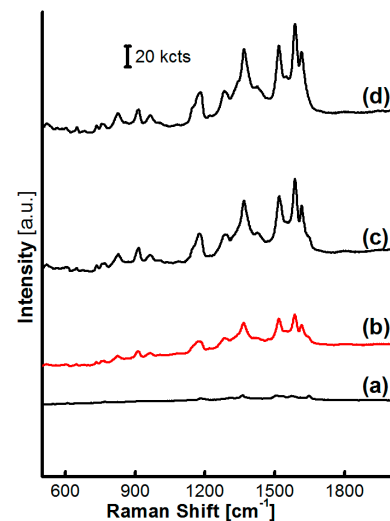


**Figure S19.** SERRS spectrum as a function of the basic violet 14 concentration on the optimized AgNP/MF<sub>6</sub>. (a)  $1.0 \times 10^{-11}$ , (b)  $1.0 \times 10^{-9}$ , (c)  $1.0 \times 10^{-7}$  and (d)  $1.0 \times 10^{-5}$  M were basic violet 14-SERRS spectra on the optimized AgNP/MF<sub>6</sub> treated with a basic violet 14 solution from  $1.0 \times 10^{-11}$  to  $1.0 \times 10^{-5}$  M basic violet 14 at a laser power of 0.01 mW. The basic violet 14 SERRS spectrum was still clear if the AgNP/MF<sub>6</sub> was treated with a  $1.0 \times 10^{-9}$  M basic violet 14 solution.